

# Simulating irradiance and color during lunar eclipses using satellite data

Stanley David Gedzelman<sup>1,3</sup> and Michael Vollmer<sup>2,\*</sup>

<sup>1</sup>Department of Earth and Atmospheric Sciences and NOAA CREST Center, City College of New York, New York, New York 10031, USA (sgedzelman@sci.ccny.cuny.edu)

<sup>2</sup>Fachbereich Technik, Brandenburg University of Applied Sciences, Brandenburg, Germany

<sup>3</sup>Department of Optics, University of Granada, Granada, Spain

\*Corresponding author: vollmer@fh-brandenburg.de

Received 29 April 2008; accepted 16 June 2008;  
posted 29 July 2008 (Doc. ID 95617); published 30 September 2008

Irradiance and color during the total lunar eclipses of 2007 and 2008 are simulated using a ray tracing model that includes refraction, scattering by molecules, and observed or climatological distributions of aerosols, ozone, clouds, and topography around the terminator. Central portions of the umbra appear deep red for almost all eclipses due to preferential removal of short wavelengths in the spectrum of sunlight by scattering in the lower troposphere. The fringe of the umbra appears turquoise or blue due to selective removal of wavelengths around 600 nm by the Chappuis absorption bands of ozone in the stratosphere. Asymmetric distributions of clouds and aerosols, particularly for the 2008 eclipse, produce minimum calculated irradiance up to 17 arc min from the umbra center, while high ozone content over the arctic makes the northern edge of the umbra deepest blue. © 2008 Optical Society of America

*OCIS codes:* 010.1110, 010.1290, 010.1615, 010.1690, 010.4950, 010.5620.

## 1. Introduction

Knowledge about lunar eclipses has been summarized in excellent papers [1,2]. Most eclipse models have treated the spherically symmetric Earth and atmosphere in large part because global measurements of relevant properties of the atmosphere such as the distributions of clouds, aerosols, and ozone have not been available and remain inadequate. Symmetric models have the advantage of simplicity and offer the ability to analyze the impact of each parameter separately, and this was the approach taken in our companion paper [3]. The models also provide results that agree crudely with the observed light curves during eclipses [4]. But spherically symmetric models invariably fail to account for observed details of eclipses. For example, they cannot reproduce any of the observed spatial asymmetries of irradiance and color in Earth's umbra.

Remote sensing techniques now provide global measurements of many atmospheric parameters that attenuate sunlight during lunar eclipses, including ozone concentrations, aerosol optical depths, cloud cover, and height, and of course, topography. These measurements have come on line only recently and offer the first opportunity to attempt to model the light and color during eclipses. Therefore, in this paper, we use values of the parameters along the terminator of the eclipses to model the irradiance and color of the total lunar eclipses of 3–4 March 2007 and 21 February 2008. But the reader should be forewarned that the measurements are still inadequate to produce accurate simulations, because they often rely on long time averages and lack critical data about vertical distributions.

The paper is organized as follows: First, we discuss the ray tracing model used to compute the irradiance and spectra of light. We then compare irradiance, spectra, and color in the umbra for idealized situations to that given by a spherically symmetric model described in the companion paper [3]. We then use

data along the terminator that are pertinent for the lunar eclipses of March 2007 and February 2008 to simulate their irradiance and spectra and discuss the results.

## 2. Ray Tracing Model for Refraction and Attenuation of Light during Lunar Eclipses

We described the geometry for the eclipse model and a spherically symmetric ray tracing model in our companion paper [3]. In brief, the irradiance and spectra at each point in the umbra are due almost entirely to direct sunlight that passed through the atmosphere. It is therefore necessary to compute the refraction and attenuation of sunlight in the atmosphere along the terminator and then integrate over the region of the atmosphere that contributes light to a given point on the Moon. Refraction depends on the pressure and vertical temperature structure along the path. Attenuation is due to scattering by air molecules, extinction by aerosols, absorption by ozone, and obstruction by topography and clouds.

The ray tracing model presented here uses the same physics as the spherically symmetric model of [3] but includes observed variations around the terminator of all relevant parameters and uses somewhat different ray tracing. For example, it represents sunlight by a Planck radiator at 5750 K, calculates spectral irradiances at 61 wavelengths in 5 nm steps from 400 to 700 nm, includes variations of the distance from Earth to Sun and to Moon, and makes similar assumptions about the vertical distributions of aerosols and ozone as in [3], because there are no regular global observations of these distributions.

The model begins by tracing a series of beams that originate in the center of the Sun and pass through minimum heights,  $z_{\min}$  along the terminator for every 100 m from  $0 \leq z \leq r_{\text{earth}}$  and for 36 equally spaced columns around the terminator. Once a beam enters the atmosphere (set at  $z = 80$  km) refraction, absorption, scattering, and extinction are calculated for steps  $dx = 100$  m until the beam reaches  $z_{\min}$ . Values of the optical air mass,  $M$ , and refraction angle,  $\psi$ , are then doubled, and the irradiance of the resulting ray is mapped onto a screen at the distance of the Moon and spread with appropriate limb darkening over a circle of radius  $r_{\text{img}}$ . This brute force approach is time consuming but includes all the geometric factors of the eclipse described in [3], such as the cross-sectional region of the atmosphere along the terminator, that contribute light to any spot in the umbra.

The optical path lengths of sunlight through the molecular atmosphere and through the ozone layer are calculated by following the refracted light beam, and the beam is attenuated by Bouguer's law. Aerosol particles are assumed to be confined to two layers, namely, 1, the atmospheric boundary layer, in which particle number density decreases exponentially with height from the ground with scale height that can be specified in the model, and 2, a layer aloft with constant number density over a thickness  $\Delta H = 1$  km at a height that can be specified in the model.

Turbidity and Ångstrom coefficient are chosen separately for each of the aerosol layers. All clouds and elevated terrain are treated as opaque barriers, as in [3], but observed variations around the terminator are included in the model of this paper.

The irradiance reaching every point on an imaginary screen at the distance of the Moon from every contributing pinhole in every column is then added to produce the irradiance within the penumbra and umbra regions on that. The light reflected from the Moon is then attenuated and tinted further on its passage down through the atmosphere, where it is recorded by an observer on Earth. Local values for the observer of the Moon's zenith angle and atmospheric turbidity and ozone content are free parameters in the model. As in [3], irradiance of forward scattered light passing through the atmosphere at the terminator and entering the umbra has been neglected as relatively tiny. As mentioned before scattering in the atmosphere serves only to diminish the irradiance of refracted sunlight reaching the umbra.

## 3. Irradiance Spectra and Color

The two most compelling features of the Moon's appearance during an eclipse are the red color of the umbra core and the blue umbral fringe; see Fig. 9. Indeed, similarity of the situations suggest that the eclipsed Moon should appear almost as red as the setting Moon seen by astronauts (where  $z_{\min} = 0$ ). Figure 1 shows spectra computed with the spherically symmetric model for a range of points that extend from the center of the umbra to the penumbra for typical eclipse conditions as observed from sea level on Earth when the Moon appears at zenith angle,  $\phi_{\text{Moon}} = 60^\circ$ . Irradiance of long visible waves in the umbra core is so dominant (but still weak) that it produces a dark brown-red appearance despite absorption of orange light by ozone, which

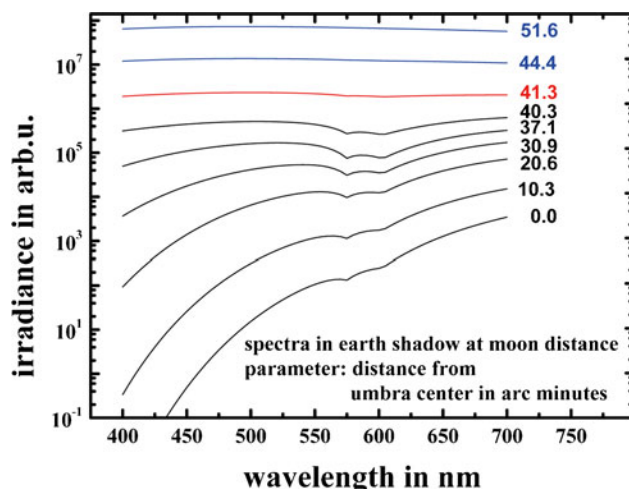


Fig. 1. (Color online) Irradiance spectra of eclipsed moonlight for points located at given distances in arc minutes from the center of the umbra as observed from Earth for typical atmospheric conditions (300 DU ozone, 1 km elevation,  $\beta = 2$ ). The penumbra begins at about 42 arc min (third line from top).

produces a prominent double dip due to the Chapuis bands at 575 and 605 nm for all spectra in the umbra. In contrast, light near the edge of the umbra ( $\approx 42$  arc min) appears turquoise or blue because it has passed well above the troposphere (e.g.,  $z_{\min} > 15$  km), where depletion of longer wavelengths by absorption exceeds the depletion of short waves by scattering. In the penumbra the spectra match the spectrum of direct sunlight seen at the Earth's surface because almost all the sunlight in the penumbra has passed above the atmosphere.

Variations of the observer's lunar zenith angle have a relatively small impact on the spectra and appearance of the eclipsed Moon to an Earthbound observer until the Moon approaches the horizon. When the Moon appears between about  $10^\circ$  and  $20^\circ$  above the horizon the major change of its appearance to an Earthbound observer is a reduction of the blue-green color near the edge of the umbra due to loss from scattering in the long oblique return path through the atmosphere. However, once the eclipsed Moon is closer to the horizon than about  $5^\circ$  or  $10^\circ$  light from the twilight atmosphere is so overwhelming that the eclipsed Moon will disappear from view.

Absorption of light around 600 nm by stratospheric ozone is responsible for the blue umbral fringe. Figure 2 indicates the color sequence from the center to the edge of the umbra for 0, 300, and 600 DU of ozone (1 DU corresponds to  $10^{-2}$  mm at standard temperature and pressure) on the 1931 CIE diagram. With zero ozone, the color grades from deep red (saturation  $> 95\%$ ) at umbra center to almost white at the edge of the penumbra. With 300 DU of ozone, the edge of the umbra is blue-green or turquoise while the center of the umbra is actually slightly redder than without ozone. This slightly deeper red color is due to the additional absorption of orange light where irradiance at short wavelengths is so small. When ozone content increases to 600 DU the umbra fringe is deep blue.

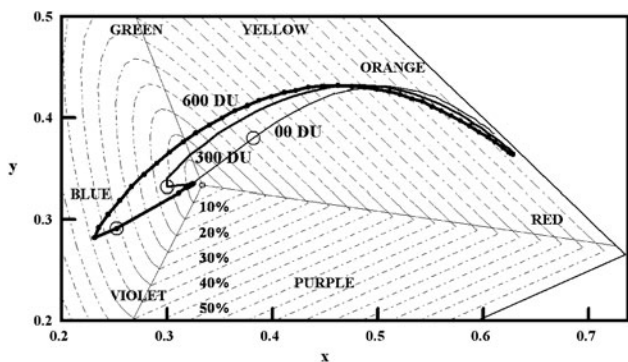


Fig. 2. CIE diagram (1931) showing the impact of ozone on the color sequence extending from the center to the outer edge of the penumbra for 0 DU (thin curve), 300 DU (middle curve), and 600 DU (thick curve with solid circles indicating points separated by 1.03 arc min starting at umbra center). The dashed contour lines represent the percentage of color saturation. The large hollow circles indicate the point just inside the border of the umbra. The achromatic white point is at  $x = y = 1/3$ .

Irradiance in the umbra is sensitive not only to the gross turbidity of the atmosphere but to the vertical distribution and mean size or Ångstrom coefficient of the aerosol particles. The great sensitivity of irradiance to the height of an elevated aerosol layer was treated in [3], and an example of how merely changing the scale height of an aerosol layer with maximum concentration at ground level is shown in Fig. 3. The three curves show calculated irradiance from the spherically symmetric model as a function of angular distance from umbra center when the sea level temperature ( $T_{sl} = 289$  K) lapse rate is  $6 \text{ K km}^{-1}$  and the tropopause is at 12 km. The top curve applies to the molecular atmosphere with no aerosols, no ozone, and no topography. The two lower curves refer to an aerosol-loaded atmosphere. Number concentration of aerosol particles is represented by the atmospheric turbidity,  $\beta$ , which is the ratio of the hazy atmosphere's total scattering cross section integrated over the visible light spectrum to that of a pure, molecular atmosphere. Thus,  $\beta = 1$  corresponds to a molecular atmosphere, and  $\beta = 2$  represents an atmosphere in which aerosols absorb and/or scatter as much sunlight when the Sun is overhead as air molecules scatter. Effective aerosol size, another free parameter, is given in terms of the Ångstrom coefficient,  $\alpha$ , where  $\tau_\lambda = \tau_{\lambda_0}(\lambda/\lambda_0)^{-\alpha}$ .

The two bottom curves of Fig. 3 represent an atmosphere with turbidity,  $\beta = 2$ , Ångstrom coefficient  $\alpha = 1$ , ozone content 300 DU, and topography or cloud cover 1 km high around the terminator. The only difference between the situations represented by the two bottom curves is the aerosol scale height, which is 2.5 km for the center curve and 5 km for the bottom curve. At umbra center irradiances of the three curves are reduced to fractions,  $4.1 \times 10^{-4}$ ,  $3.3 \times 10^{-5}$ , and  $8.2 \times 10^{-6}$ , of uneclipsed moonlight. Merely doubling scale height without changing aero-

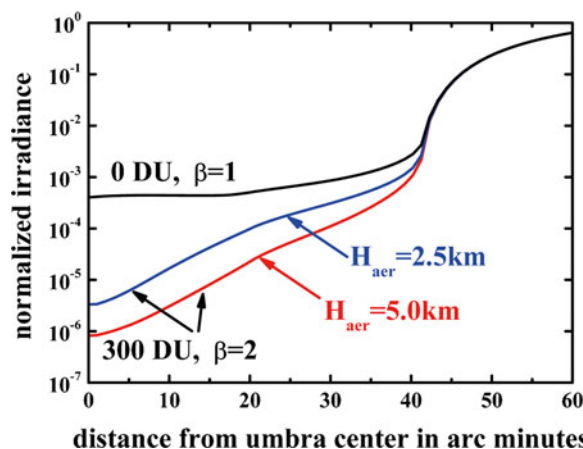


Fig. 3. (Color online) Irradiance of moonlight relative to that of the uneclipsed Moon as a function of angular distance in minutes from umbra center. The top curve applies to a molecular atmosphere with no aerosols, ozone, or topography. The bottom two curves have turbidity  $\beta = 2$ , ozone column content = 300 DU, and uniform topography 1 km high. The center and bottom curves have aerosol scale heights of 2.5 and 5.0 km, respectively.

sol column content reduces irradiance by an additional factor of about 4. An elevated aerosol layer with the same optical depth  $\tau$  would reduce irradiance even more drastically because the optical air mass is larger for thinner elevated layers.

Major volcanic eruptions have long been known to greatly darken and possibly redden the eclipsed Moon [5,6]. Their impact can be simulated by introducing a stratospheric aerosol layer. Figure 4 shows the impact of three aerosol layers, each with different effective particle size characterized by the Ångström coefficient  $\alpha = 1, 0,$  and  $-1$  [3]. The layers are centered at  $H = 18$  km with turbidity  $\beta = 1.5$  at umbra center and fringe. The elevated layers reduce irradiance at all wavelengths by at least an order of magnitude, but what may be surprising at first is the great sensitivity of irradiance to the Ångström coefficient. The volcanic stratospheric particles responsible for red twilights ( $\alpha = -1$ ) are most effective in extinguishing light in the umbra because they are most efficient at scattering the long waves of sunlight, i.e., the waves that manage to penetrate the lower troposphere without being scattered severely. Thus, even with a turbidity of  $\beta = 1.5$  ( $\tau \approx 0.05$ ), a stratospheric aerosol layer with  $\alpha = -1$  will reduce irradiance in the center of the umbra by a factor of from  $10^2$  at  $\lambda = 700$  nm to  $10^4$  at  $\lambda = 400$  nm. Smaller aerosol particles in the stratosphere are considerably less effective at reducing irradiance near the center of the umbra because they scatter primarily the shorter wavelengths already scattered away in the troposphere. Near the fringe of the umbra the size of stratospheric aerosol particles has almost no impact on the irradiance so long as most of the aerosols lie below the ozone layer.

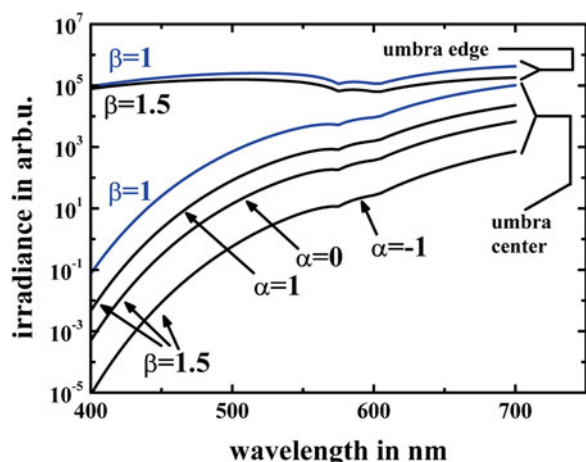


Fig. 4. (Color online) Spectral irradiance of eclipsed moonlight at the center (angular distance from center  $\phi = 0'$ ) and near the fringe of the umbra ( $\phi = 40.3'$ ) due to aerosol layers with turbidity  $\beta = 1.5$  centered at a height of 18 km for Ångström coefficients  $\alpha = -1, 0,$  and  $1$  as seen from Earth for 300 DU ozone and 0 km elevation.

#### 4. Simulation of the Lunar Eclipses of 3–4 March 2007 and 21 February 2008

The appearance of the Moon during lunar eclipses can be simulated by incorporating accurate measurements of topography, cloud cover, and heights, as well as ozone and aerosol concentrations and height distributions. Aerosols and ozone have an influence both at the location of the Earthbound observer and along the terminator. Here, we attempt to simulate the appearance of the umbra for the total lunar eclipses of 3–4 March 2007 and 21 February 2008. However, be aware that our results are at best suggestive. As we have shown the great sensitivity of irradiance to changes in the horizontal and vertical distributions of clouds, aerosols, and ozone (which can vary in short times, and which are not well known) have enormous impact on the light and color of the eclipsed Moon.

Because the Moon can be viewed from almost half the world, its color and brightness during an eclipse depend on the values of surface pressure, lunar zenith angle, atmospheric turbidity, and ozone content at the observer's location. All these are free parameters in the model. The conditions we used to model the eclipses along the terminator represent a combination of satellite data and default values for a number of meteorological variables. Temperature structure, height, and width of the ozone layer and aerosol layer all default to climatological means. Sea level temperature was set to range from 300 K at the equator to 240 K at the polar edges of the terminator, while tropopause height is 17 km over the equator, 7 km over the poles, and 12 km at  $45^\circ$  latitude, where it slopes most steeply. The tropospheric lapse rate was set to  $6 \text{ K km}^{-1}$ . The ozone layer was centered 9 km above the tropopause as a bell-shaped curve with a full width at half-maximum of 20 km but decreased abruptly to 10% of its maximum value in the troposphere. Aerosol concentration was assumed to be greatest at ground level and decreases exponentially with a scale height of 2.5 km. Thus, elevated aerosol layers and their strong extinguishing impact on umbral light were neglected.

Each of the measured parameters has limited accuracy for several reasons. The first source of errors was that values of the parameters were determined subjectively from the global images posted on the internet in each of 36 equally spaced bands around the terminator. Second, the terminator was set using the "greatest" or darkest time of the eclipse even though during the 60 to 100 min period of totality the terminator ranges as much as  $7.5^\circ$  to  $12^\circ$  about its central longitude. Third, potentially large errors result from the large averaging times of the satellite data needed for global coverage, which range from about 6 to 12 h for clouds and up to 1 month for aerosols.

Daily global maps of total column ozone are provided by the Canadian ozone and ultraviolet measurement program [7]. These maps are blended products derived from many satellites such as the Total Ozone Mapping Spectrometer (TOMS). Ozone

soundings are generally not available, but model calculations indicate that irradiance is relatively insensitive to changes in ozone height distributions. Irradiance increases by 10% at the center and 3% near the edge of the umbra as the height of the ozone layer rises from 16 to 26 km. The major difference is that the higher ozone layer produces a distinctly bluer fringe of the umbra.

Figure 5 shows the total column ozone for 3 March 2007 and 21 February 2008, the days of total lunar eclipses. The black lines show the approximate positions of the terminators near eclipse maximum. The terminator location was calculated based on data at eclipse maximum taken from [8]. The two ozone maps share several general features such as the maximum at high boreal latitudes and minimum in the tropics, but quantitative differences between the two days are quite large. The highest ozone totals along the northernmost sections of the terminators reach values as large as 600 DU for the 2007 eclipse but only 475 DU for the 2008 eclipse. Because the Moon passed near the northern edge of the umbra during the 2007 eclipse and the southern edge in the 2008 eclipse, the blue color when the Moon entered the umbra in the 2007 eclipse should have been much deeper and wider. In any case, the generally high ozone totals in the higher latitudes of the North



Fig. 5. (Color online) Maps of ozone concentration for the 2007/03/03 and 2008/02/21 eclipses after [http://exp-studies.tor.ec.gc.ca/e/ozone/Curr\\_allmap\\_g.htm](http://exp-studies.tor.ec.gc.ca/e/ozone/Curr_allmap_g.htm). The thick black dotted lines represent the terminators at the peak of the eclipses.

Hemisphere during its spring can produce the purest blues in any eclipse for which the Moon passes through the northern border of the umbra.

As noted earlier, data for aerosols are much less satisfactory and lack of knowledge of the vertical distribution has much more serious consequences for irradiance during lunar eclipses. Global maps of mean monthly aerosol optical depths (AODs) for both blue and red light are available from NASA's Multiangle Imaging Spectroradiometer (MISR) [9]. The satellite covers the Earth every 9 days, and Level 3 data are provided for AOD for blue ( $\lambda_{\text{ctr}} = 446.4 \text{ nm}$ ,  $\sigma_{\lambda} = 41.9 \text{ nm}$ ) and red ( $\lambda_{\text{ctr}} = 671.7 \text{ nm}$ ,  $\sigma_{\lambda} = 21.9 \text{ nm}$ ) light. AOD values  $\tau_{\text{Aer}}$  for blue light are converted to value of turbidity,  $\beta$ , for use in the model by  $\beta = 1 + \tau_{\text{Aer}}/\tau_{\text{Mol}}$  with  $\tau_{\text{mol}}(\lambda = 446 \text{ nm}) = 0.19$ .

Even though global aerosol patterns show considerable consistency, monthly average values are only suggestive of conditions during the eclipse. MODIS satellites [10] provide global maps of daily, 8 day, and monthly AODs (at  $\lambda_{\text{ctr}} = 550 \text{ nm}$ ), but with larger data gaps at the shorter time intervals. The map for March 2007 (Fig. 6) reveals high values of AOD over Equatorial West Africa extending westward over the Atlantic as a result of dust transported from the Sahara Desert, and over and downwind from Southeast Asia, particularly India and China. Lowest values occur in the subtropical oceans, with a band

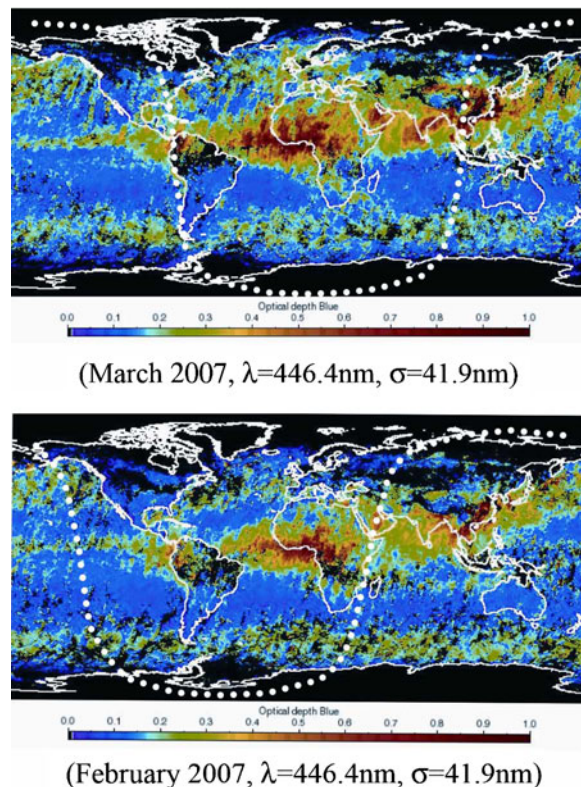


Fig. 6. (Color online) Global map of aerosol optical depth (AOD) for blue light ( $\lambda = 446 \text{ nm}$ ) for March 2007 and February 2007 after [http://eosweb.larc.nasa.gov/PRODOCS/misr/level3/level3\\_CGAS\\_small.html](http://eosweb.larc.nasa.gov/PRODOCS/misr/level3/level3_CGAS_small.html). The thick white dotted lines are the terminators for the March 2007 and February 2008 eclipses.

of somewhat elevated optical depths over the storm belt of the South Hemisphere Oceans. Data are missing in the high latitudes. For the February 2008 eclipse, the monthly global aerosol map was not available so we used the aerosol map for February 2007.

As with the global ozone maps, global aerosol maps are column totals and give no information about the vertical distribution. Our typical assumption that aerosol concentration decreases exponentially upward from ground level with a scale height of 2.5 km amounts to confining most aerosols near the ground, where the effective optical thickness of the molecular atmosphere is so great that little light would reach the Moon even without aerosols. But satellites and vertically pointing lidars reveal the frequent presence of elevated dust and aerosol layers [11,12] transported over great distances, such as dust from the Sahara or Gobi Deserts, and stratospheric aerosol layers cover the globe after large volcanic eruptions such as Pinatubo in 1991.

Similarly large errors can arise from clouds' highly variable effects on the irradiance and color of lunar eclipses. We treat all clouds as opaque barriers to light passing through the atmosphere at the terminator (see Fig. 8(b) in [3]). We used images and cross sections of CloudSat [13] to determine cloud cover and top heights. Because the International Satellite Cloud Climatology Project (ISCCP) often does not detect clouds with vertical optical depths  $\tau_n \leq 0.1$  [14], high thin cloud layers can block tangentially incident light as effectively as elevated aerosol layers and thus can reduce irradiance near umbra center by an order of magnitude.

Several other sources of error arise when considering clouds. Cloud cover was taken along the terminator from the image at the time of the eclipse maximum (Fig. 7). Since the satellite is a near polar orbiter and flies in a Sun synchronous orbit near local noon, cloud heights at the terminator either lag or lead eclipse maximum by about 6 h. During this time interval, changes of cloud heights are generally small for the stratiform clouds of extratropical weather systems but can be large for convective clouds. Each band was treated as overcast if cloud cover was greater than or equal to 50% and treated as clear otherwise. Fields of convective clouds were treated as if they were overcast because horizontal light beams are invariably blocked by one cloud or another. Finally, the terminator is not a line but a broad band about 800 km wide for clouds and aerosol layers 10 km high. Clouds or aerosols anywhere in such a band will reduce irradiance in the umbra.

Despite all the limitations, there is much value in attempting to simulate actual eclipses because at least some of the major qualitative features of the Moon's appearance will be captured, such as the color and asymmetries of irradiance. Figure 8 gives the normalized irradiance in simulated EW and NS sections (based on Earth geography) through the umbra center for the 3–4 March 2007 lunar eclipse. It is based upon the measurements and values of topogra-

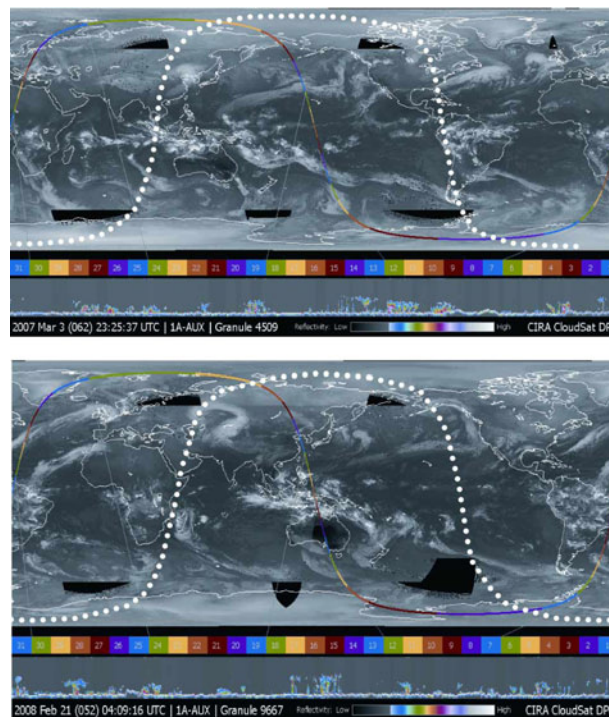


Fig. 7. (Color online) CloudSat images at 2325 UTC 3 March 2007 and 0409 UTC 21 February 2008 near eclipse maximum (after <http://www.cloudsat.cira.colostate.edu/>). The thick white dotted lines represent the terminator at the eclipse maxima. The colored line shows the satellites' orbit. The cross sections with a vertical scale of 30 km show cloud reflectivity and topography at the bottom of each panel. More detailed views of each colored section are available from the authors.

phy, temperature, cloud cover, and height as well as aerosol and ozone contents described above.

Simulated irradiances near the umbra center for both the 2007 and the 2008 eclipses are more than an order of magnitude higher than in Fig. 3. Since the latter nearly coincided with measured brightness during the 1990 and 2007 lunar eclipses [4], the irradiance data of Fig. 8 are much too large, most likely

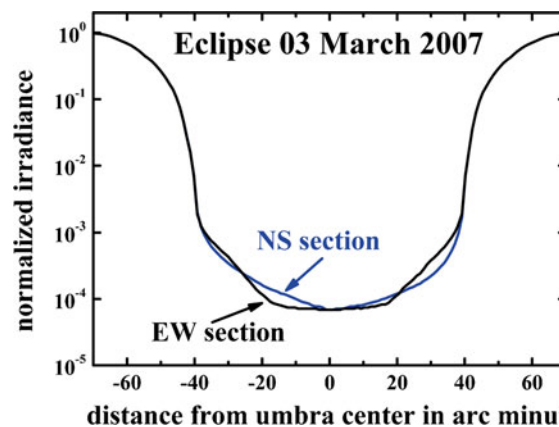


Fig. 8. (Color online) EW and NS sections of calculated values of normalized irradiance through the umbra center for the total lunar eclipse of 3 March 2007.

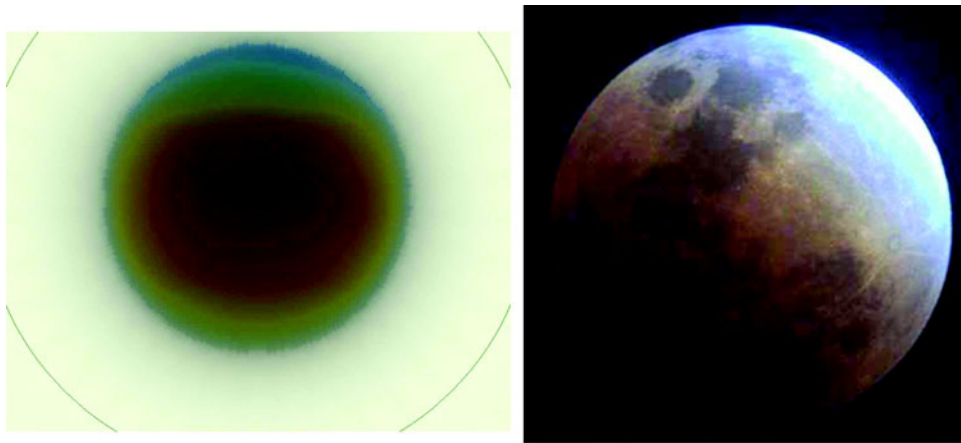


Fig. 9. Simulated color image of umbra for conditions of eclipse of 3–4 March 2007 (left) and a photograph of the Moon at the edge of the umbra during the February 2008 eclipse by [16] (right).

because of the neglect of both high, thin clouds and elevated aerosol layers.

For the 2007 eclipse, Fig. 8 shows that calculated irradiances in both the EW and NS planes were reasonably symmetric around the umbra center, although somewhat lower values occur at the north edge of the umbra due to greater aerosol content and much higher ozone content in the North Hemisphere.

The major difference between the North and the South Hemispheres can be seen in the simulated color image of the March 2007 eclipse (Fig. 9, left) and the CIE diagram showing color through the NS section of the umbra (Fig. 10). The blue color inside the edge of the umbra is widest and most pronounced at the northern edge of the umbra because of the extremely high ozone content along the northern section of the terminator. The southern and equatorial fringes of the umbra are turquoise at best and narrower.

Calculated irradiance for the 21 February 2008 eclipse was notably asymmetric, particularly in the EW plane (Fig. 11). The asymmetry was caused by persistently greater aerosol content and cloud cover and higher clouds along the stretch of the terminator that crossed Eastern Africa, the Arabian Desert, and Central Asia than along the stretch that crossed over

the central Pacific Ocean. As a result minimum irradiance was calculated to occur 17 arc min from the umbra center. Such asymmetric irradiance distributions may account for most of the observed brightness asymmetries during total lunar eclipses [15].

Furthermore, because the lowest ozone content occurs in the tropics (except for the ozone hole of the Austral spring) eclipses that run through the center of the umbra will not only tend to get darkest and deepest red at the eclipse maximum but will also tend to be least blue when they enter and exit the umbra. It would be interesting to see whether the turquoise fringe is absent for eclipses that run through the southern edge of the umbra during the Austral spring, when the ozone hole is deepest. The symmetric model indicates the turquoise fringe vanishes once column ozone content is less than about 150 DU.

## 5. Summary and Conclusions

In this paper, we used an eclipse model to simulate the well-known deep red color of the Moon when near the center of the umbra and the turquoise or blue col-

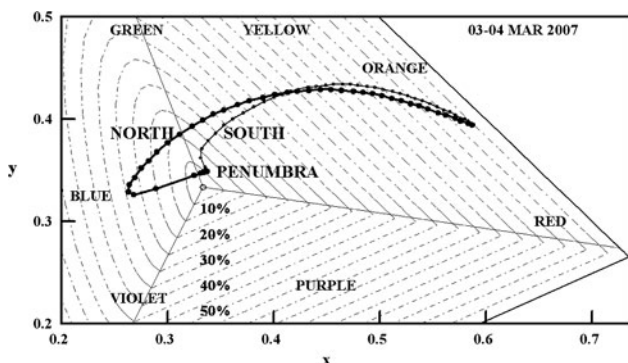


Fig. 10. CIE diagram (as in Fig. 2) of simulated colors of the NS section of the umbra through umbra center for the eclipse of 3–4 March 2007. The thick line indicates points north of the center. The circles are separated by 1.03 arc min.

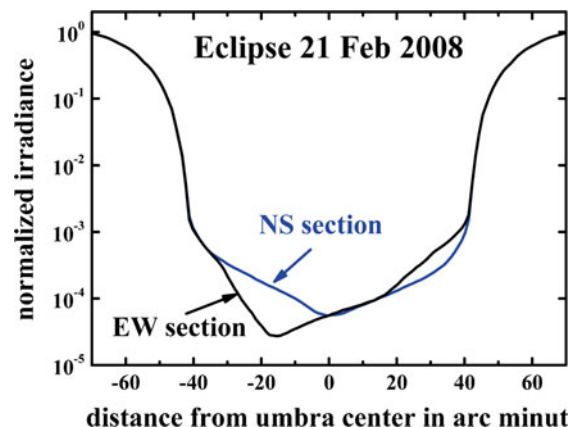


Fig. 11. (Color online) EW and NS sections of calculated values of normalized irradiance through the umbra center for the total lunar eclipse of 21 February 2008. Minimum irradiance for the EW section occurs about 17 arc min from the umbra center.

or for the part of the Moon just inside the edge of the umbra during total lunar eclipses. The model utilized a mixture of observations of cloud cover and heights, topography, column aerosol, and ozone amounts with climatological means of temperature and vertical distributions of aerosols and ozone to simulate the total lunar eclipses of 3–4 March 2007 and 21 February 2008. Calculated irradiance fell to less than  $10^{-4}$  that of the fully sunlit Moon in the center of the umbra, but the distribution of irradiance and color was asymmetric because of large observed variations of topography, cloud cover, ozone content, and aerosol content around the terminator.

Unfortunately, with the data now available it remains impossible to simulate accurately the light and color during lunar eclipses. Timely and critical quantitative global data about the nature and height distribution of aerosol particles, ozone, and clouds at the time of the eclipse is lacking. Light and color in the umbra exhibits great sensitivity to these parameters and can produce errors in calculated irradiance of more than an order of magnitude. Even so, simulations of eclipses that use available data have value because they can capture some of the observed features of particular lunar eclipses. Among these are asymmetries in irradiance and variations of the width and color purity of the blue region of the Moon when it appears near the fringe of the umbra. And, when accurate data about the relevant atmospheric properties become available, the model presented here should provide accurate simulations of the light and color during total lunar eclipses.

S. D. Gedzelman gratefully acknowledges support by a National Oceanic and Atmospheric Administration (NOAA) CREST grant, by a Professional Staff Congress City University of New York (PSC CUNY) grant, and by the Department of Optics at the University of Granada. M. Vollmer thanks the German Science Foundation (DFG) for travel grants to international conferences in the field.

## References

1. F. Link, "Lunar eclipses," in *Physics and Astronomy of the Moon*, Z. Kopal, ed., 1st ed. (Academic, 1962), pp. 161–229, more recent mostly identical version in Z. Kopal, ed., *Advances in Astronomy and Astrophysics* (Academic, 1972), Vol. 9, pp. 68–144.
2. A. Mallama, *Eclipses, Atmospheres and Global Change*, self-published, 1996, contact Anthony\_Mallama@raytheon.com
3. M. Vollmer and S. D. Gedzelman, "Simulating irradiance during lunar eclipses: the spherically symmetric case," *Appl. Opt.* **47**, H52–H61 (2008).
4. N. Hernitschek, E. Schmidt, and M. Vollmer, "Lunar eclipse photometry: absolute luminance measurements and modeling," *Appl. Opt.* **47**, H62–H71 (2008).
5. R. A. Keen, "Volcanic aerosols and lunar eclipses," *Science* **222**, 1011–1013 (1983).
6. "Danjon scale for lunar eclipses," <http://eclipse.gsfc.nasa.gov/OH/Danjon.html>
7. WMO/GAW World Ozone and UV Radiation Data Centre (WOUDC), "Environmental Canada, Ozone Maps," [http://exp-studies.tor.ec.gc.ca/e/ozone/Curr\\_allmap\\_g.htm](http://exp-studies.tor.ec.gc.ca/e/ozone/Curr_allmap_g.htm)
8. <http://sunearth.gsfc.nasa.gov/eclipse/eclipse.html>
9. NASA Langley Research Center, "Atmospheric Science Data Center, MISR Data and Information: Data Products," <http://eosweb.larc.nasa.gov/>.
10. "MODIS Atmosphere: Aerosol," <http://modis-atmos.gsfc.nasa.gov/>.
11. D. Müller, I. Mattis, A. Ansmann, U. Wandinger, and D. Althausen, "Raman lidar observations of aged Siberian and Canadian forest fire smoke in the free troposphere over Germany in 2003: Microphysical particle characterization," *J. Geophys. Res.* **110**, D17201 (2005).
12. J. M. Prospero and J. P. Lamb, "African droughts and dust transport to the Caribbean: climate change, and implications," *Science* **302**, 1024–1027 (2003).
13. "CloudSat Data Processing Center," <http://www.cloudsat.cira.colostate.edu/>.
14. W. B. Rossow and R. A. Schiffer, "Advances in understanding clouds from ISCCP," *Bull. Am. Meteorol. Soc.* **80**, 2261–2286 (1999).
15. R. Gerharz, "Photometric brightness asymmetry during a lunar eclipse," *Arch. Meteorol. Geophys. Bioklimatol., Ser. A* **18**, 221–226 (1969).
16. "Photo Gallery: Total Lunar Eclipse, 2-20-2008," <http://www.skyandtelescope.com/community/gallery/skyevents/15836532.html>, photographer B. Johnson.